# Three-dimensional Reconstructed Contrast–enhanced MR Angiography for Internal Iliac Artery Branch Visualization before Uterine Artery Embolization

Nagy N.N. Naguib, MSc,* Nour-Eldin A. Nour-Eldin, MSc,* Renate M. Hammerstingl, MD, Thomas Lehnert, MD, Julius Floeter, MD, Stefan Zangos, MD, and Thomas J. Vogl, MD

**PURPOSE:** To evaluate the feasibility of three-dimensional (3D) reconstructed contrast-enhanced (CE) magnetic resonance (MR) angiography in mapping the pelvic arteries in women before uterine artery embolization (UAE).

**MATERIALS AND METHODS:** CE MR angiography studies before UAE in 49 women (age range, 38–57 years; mean, 47.04 y ± 4.7 [SD]) who underwent UAE for uterine leiomyomas between February 2005 and February 2007 were retrospectively evaluated by two radiologists in consensus. Studies were performed on a 1.5-T MR unit with a 3D fast low-angle shot sequence in the coronal direction. Reconstruction was performed with 3D computed tomographic angiography reconstruction software.

**RESULTS:** In the current study, 98 internal iliac arteries (IIAs) from 49 women were studied. The superior and inferior gluteal arteries were visualized in all cases ($N = 98$; 100%), the lateral sacral artery in 86 cases (88%), the iliolumbar artery in 84 (86%), the obturator artery in 81 (83%), the internal pudendal artery in 96 (98%), and the uterine artery in 95 (97%). The superior vesical and middle rectal arteries were seen in 21 (21%) and 11 (11%) cases, respectively. The mean length of the uterine artery was 12.56 cm (range, 4.6–22.2 cm), and it showed the longest traceable length among all branches. The uterine artery showed five patterns of origin. The superior gluteal artery showed constant origin from the posterior division of the IIA, whereas the iliolumbar and obturator arteries showed the most variations in origin.

**CONCLUSIONS:** Three-dimensional reconstructed CE MR angiography can detect most branches of the IIA in addition to their point of origin. Therefore, it can be used as a mapping tool of the pelvic arterial tree before UAE.

**J Vasc Interv Radiol 2008;** 19:1569–1575

**Abbreviations:** CE = contrast-enhanced, IIA = internal iliac artery, 3D = three-dimensional, UAE = uterine artery embolization

THE internal iliac artery (IIA) can be regarded as a silent artery in women. In male subjects, it gains its importance from the possibility of being a cause of vasculogenic impotence (1). Apart from this, its disease entities usually—but not always (2)—remain asymptomatic except when the IIA is acutely occluded or an aneurysm develops (which might present with pelvic mass, pain, and/or sudden rupture). This probably results from the presence of an excellent network of collateral vessels in the pelvis that can be used in case of stenosis or obstruction. Even IIA occlusion can be used as a treatment for some gynecologic conditions (3,4) or as a part of endovascular repair of abdominal aortic aneurysms (5–7).

Uterine leiomyomas (or fibroid tumors) are the most common pelvic tumors, with an overall incidence of 35%–50% among all women (8). Uterine artery embolization (UAE) is a minimally invasive therapy for uterine leiomyomas that represents an alternative to hysterectomy and myomectomy (9), or it can be performed before myomectomy as a part of combined therapy aimed at reducing the bleeding during multiple myomectomy operation. During the past decade, UAE has been established as a safe and effective first-line therapy for the treatment of symptomatic leiomyomas in premenopausal women (10). How-

From the Institute for Diagnostic and Interventional Radiology, Johann Wolfgang Goethe University Frankfurt, Theodor-Stern-Kai 7, 60590 Frankfurt am Main, Germany. Received March 3, 2008; final revision received and accepted August 8, 2008. **Address correspondence to** N.N.N.N.; E-mail: nagynnn@yahoo.com

*Drs. Naguib and Nour-Eldin contributed equally to this work.

None of the authors have identified a conflict of interest.



**DOI: 10.1016/j.jvir.2008.08.012**

ever, the pelvic arterial anatomy is among the most complex in the body. Identifying and catheterizing the correct artery for UAE can be extraordinarily difficult, even for a physician who routinely does so (11). Magnetic resonance (MR) imaging is increasingly being used to evaluate patients before UAE because of its precision in helping determine the size and location of uterine leiomyomas and helping exclude other diseases (12,13).

Because of the increased popularity of pelvic interventional procedures—with UAE currently being the most common—and because of the lack of sufficient data in the medical literature regarding the study of the IIA with MR angiography, even routine angiographic studies are seen as insufficient. The present study was conducted with the aim of evaluating the feasibility of 3D reconstructed contrast-enhanced (CE) MR angiography in visualizing the different branches of the IIA and to study the anatomic variations in origin of the different branches of the IIA in women, with special emphasis on the uterine artery as the target artery in UAE.

## MATERIALS AND METHODS

The study was approved by the institutional review board. Informed consent was obtained from all patients included in the study after a full explanation of the procedure. Preembolization CE MR angiographic studies from 49 women who underwent UAE for uterine leiomyomas during the time period from February 2005 until February 2007 (age range, 38–57 years; mean, 47.04 y $\pm$ 4.7 [SD]) were retrospectively evaluated by two radiologists. All patients underwent MR imaging, including CE MR angiography, as a part of the preinterventional workup.

### Patient Selection

All patients self-reported symptomatic uterine leiomyomas. Symptoms were mainly in the form of abnormal uterine bleeding, bulk-related symptoms, pain, or a combination of symptoms. The leiomyomas were determined to be the cause of symptoms in all patients. All patients had previously undergone gynecologic examination, routine examination of clinical history, and physical examination. All patients expressed a desire to avoid surgical treatments and were extensively counseled as to the known risks and benefits of UAE and alternative treatments.

### MR Imaging and Image Reconstruction Technique

CE MR angiography was performed with a 1.5-T MR imaging system (Magnetom Symphony; Siemens, Erlangen, Germany). A body-array coil was used to cover the volume of interest. First, gradient-echo magnetization-transfer scout images (echo/repetition times, 5/15 msec; 40° flip angle; slice thickness, 10 mm; matrix, 128 $\times$ 256, 40-cm field of view) were obtained in three planes. Second, T2-weighted single-shot turbo spin-echo MR images (echo/repetition times, 95/4,000 msec; 150° flip angle, slice thickness, 6 mm; matrix, 128 $\times$ 256; 35-cm field of view) were obtained in the sagittal direction. Before application of the contrast agent, an unenhanced 3D fast low-angle shot sequence (echo/repetition times, 1.28/3.66 msec; 25° flip angle, slice thickness, 1.2 mm; matrix, 128 $\times$ 512, 40-cm field of view) in a coronal slice orientation was performed during the end-inspiratory phase. The study should extend anteriorly to include the external iliac artery and its inferior epigastric branch and should extend posteriorly to include the inferior gluteal and internal pudendal arteries at the point where they escape from the pelvis between the piriforms and coccygeus muscles (this is the most posterior point along their course). For the determination of the travel time for contrast material from the injection site to the pelvic vessels, a test bolus technique was used. Two milliliters of gadopentetate dimeglumine (Magnevist; Schering, Berlin, Germany) were used for this purpose. Patients' renal function was checked before contrast agent administration. Based on the circulation time, contrast agent was intravenously injected (0.1 mmol/kg body weight followed by 20 mL normal saline solution) with an MR-compatible power injector (Spectris; Medrad, Pittsburgh, Pennsylvania) at a flow rate of 3 mL/sec. The CE MR angiography was performed with 3D fast low-angle shot acquisition, with identical imaging parameters as the unenhanced acquisition, in the arterial and venous phases. The unenhanced examination was performed to permit image subtraction of the unenhanced images from the CE images after the examination. The subtracted images obtained in the arterial phase were loaded into the multislice CT console (Somatom Sensation; Siemens), and a 3D reconstructed view of the pelvic arterial tree was obtained with use of the same software used for 3D reconstruction of the CT angiography images (Syngo Vessel View Application; Siemens). This allowed the free rotation of the 3D model in all directions to aid correct judgment of the course of the vessels in all directions.

### Image Evaluations

All MR images were assessed in consensus by two senior radiologists with more than 5 and 15 years, respectively, of experience in the field of pelvic MR imaging, who were blinded to the conventional angiographic images of the patients at the time of evaluation. For each study, nine branches of the IIA (superior and inferior gluteal, internal pudendal, iliolumbar, lateral sacral, obturator, uterine, superior vesical, and middle rectal arteries) were evaluated on each side. Branches were identified based on their course, with continual rotation of the 3D reconstructed model of the pelvic arterial tree in all directions. Each branch was evaluated for its visualization, length, and site of origin. For visualization, a three-grade scoring system was adopted: a score of 0 indicated that the artery was not seen, interrupted, or its origin could not be identified; a score of 1 indicated that the artery was faintly seen but could be traced and had no missing segments until its first branch arose; and a score of 2 indicated that the artery was clearly seen. Regarding the lengths of the branches, measurement started from their point of origin until their first branch arose or they were no more visualized.

### Data Collection and Statistical Analysis

Results of image evaluations were tabulated to facilitate their analysis and were gathered together in a single table. Regarding the degree of visual-

**Table 1**
**Score for Visualization of Each of the Studied Branches of the IIA**

| | Score | | |
|---|---|---|---|
| Branch (Artery) | 2 | 1 | 0 |
| Superior gluteal | 98 | 0 | 0 |
| Inferior gluteal | 97 | 1 | 0 |
| Lateral sacral | 58 | 28 | 12 |
| Iliolumbar | 63 | 21 | 14 |
| Obturator | 42 | 39 | 17 |
| Internal pudendal | 90 | 6 | 2 |
| Uterine | 87 | 8 | 3 |
| Superior vesical | 10 | 11 | 77 |
| Middle rectal | 8 | 3 | 87 |

ization, the sensitivity of 3D reconstructed CE MR angiography in detecting the different branches was calculated based on the assumption that all branches anatomically exist in all patients. Regarding the measured lengths of the different branches, for each branch, the mean length and SD were calculated. Finally, the exact origin of each branch was reported, with calculation of the percentage for each point of origin. All statistical evaluations were performed using BiAS software (Epsilon-Verlag, Darmstadt, Germany).

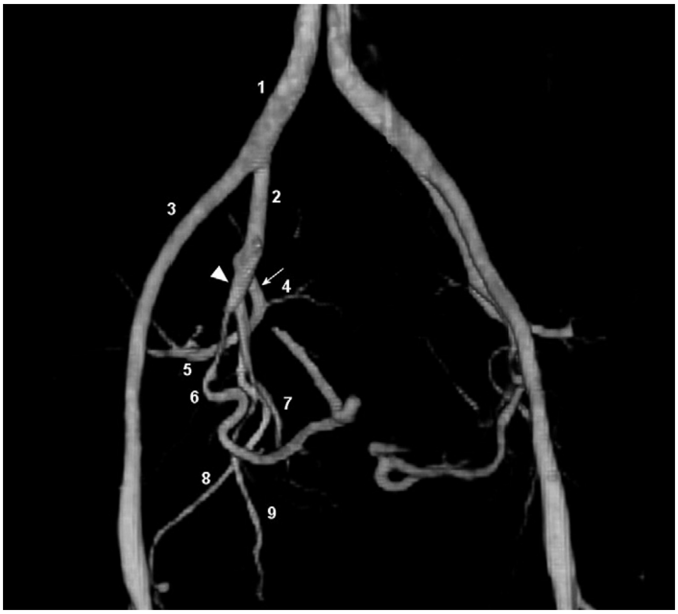


**Figure 1.** Three-dimensional reconstructed CE MR angiography image from the preembolization study of a 47-year-old woman. The model was slightly rotated toward the right side for better visualization of the arteries on the right side, namely the common iliac artery (*1*), IIA (*2*) with its anterior (arrowhead) and posterior (arrow) divisions, external iliac artery (*3*), lateral sacral artery (*4*), superior gluteal artery (*5*), uterine artery with its characteristic tortuous course originating directly from the anterior division (*6*), middle rectal artery (*7*), inferior gluteal artery (*8*), and internal pudendal artery (*9*).

## RESULTS

### Arterial Visualization

The study included CE MR angiography studies from 49 patients (98 IIAs) before UAE. **Table 1** summarizes the scores of the studied branches. Among the 98 arteries studied, the uterine artery was clearly detected (ie, score of 2) in 87 and faintly seen (ie, score of 1) in eight. The uterine artery was given a score of 0 in three arteries. The IIA gives off six parietal branches and three visceral branches. For the parietal branches, the superior and inferior gluteal arteries were visualized in all arteries studied, with an overall sensitivity of 1 for each of them. Regarding the other four parietal branches—namely the lateral sacral artery, iliolumbar artery, internal pudendal artery, and obturator artery—3D reconstructed CE MR angiography showed them with overall sensitivities of 0.88, 0.86, 0.98, and 0.83, respectively. Three-dimensional reconstructed CE MR angiography showed the visceral branches—namely the uterine artery, superior vesical artery, and middle rectal artery (**Fig 1**)—with overall sensitivities of 0.97, 0.21, and 0.11, respectively.

### Detectable Lengths

**Table 2** summarizes the lengths (range, mean, and SD) of the studied branches of the IIA. The uterine artery showed the maximum traceable length, reaching 22.2 cm; this was followed by the internal pudendal and obturator arteries with maximum lengths of 15.3 cm and 11.2 cm, respectively. The least detectable lengths were visualized in the lateral sacral and iliolumbar arteries and were 0.5 cm and 0.4 cm, respectively.

### Branch Origin

The detectable uterine arteries showed an origin from the anterior division in 86 cases (90%), from the main stem in two (2%), from the point of bifurcation of the IIA in one (1%), from the posterior division in one (1%; **Fig 2a**), and indirectly from the anterior division through a short common stem with other arteries in five (6%); four of these stems were shared with the obturator artery and one with the internal pudendal artery (**Fig 3**). The superior gluteal artery (**Fig 4a**) showed a constant origin from the posterior division of the IIA in all studied arteries, and the inferior gluteal artery originated from the anterior division in 83 of the studied arteries (85%) and from the posterior division in 15 (15%). The detected lateral sacral arteries showed an origin from the posterior division in 78 cases (91%), from the main stem of the IIA in six (7%), from the anterior division in one (1%), and from the inferior gluteal artery originating from the posterior division in one (1%). The detectable iliolumbar arteries originated from the main stem of the IIA in 42 cases (50%), from the posterior division in 37 (44%), and from the point of IIA bifurcation in five (6%). The detectable superior vesical artery (**Fig 4b**) and middle rectal artery showed a constant origin from the anterior division (100%). The detectable internal pudendal arteries showed origins from the anterior division in 91 cases (95%), indirect origin from the anterior division in three (3%), from the main stem in one (1%), and from the posterior

**Table 2**
**Detectable Lengths of the Studied Branches of the IIA**

| | Length (cm) | |
|---|---|---|
| Branch (Artery) | Range | Mean ± SD |
| Superior gluteal | 1.4–6.9 | 3.96 ± 1.03 |
| Inferior gluteal | 1.3–13 | 5.96 ± 2.56 |
| Lateral sacral | 0.5–5.6 | 2.84 ± 1.17 |
| Iliolumbar | 0.4–6 | 1.47 ± 0.85 |
| Obturator | 3.6–11.2 | 7.18 ± 1.62 |
| Internal pudendal | 1.2–15.3 | 7.9 ± 2.7 |
| Uterine | 4.6–22.2 | 12.56 ± 3.78 |
| Superior vesical | 3.2–9 | 6.12 ± 1.72 |
| Middle rectal | 0.8–7.8 | 3.52 ± 2.15 |

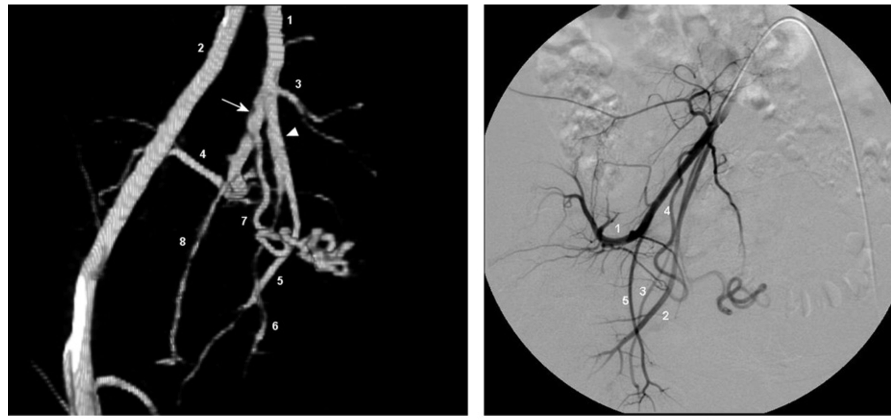

a. b.

**Figure 2.** **(a)** Three-dimensional reconstructed CE MR angiography image from the preembolization study of a 44-year-old woman. The left IIA and external iliac artery with their branches were masked and the model was rotated toward the right side for better visualization of the arteries on the right side, namely the IIA (*1*) with its anterior division (arrowhead), external iliac artery (*2*), lateral sacral artery (*3*), superior gluteal artery (*4*), inferior gluteal artery (*5*), internal pudendal artery (*6*), uterine artery (*7*) originating from the posterior division of the IIA (arrow), and the obturator artery, which also originated from the posterior division (*8*). **(b)** Angiographic image of the same patient in almost the same projection as the 3D reconstructed CE MR angiography model shows the superior gluteal artery (*1*), inferior gluteal artery (*2*), internal pudendal artery (*3*), uterine artery (*4*), and obturator artery (*5*).

division in one (1%). Last, the detectable obturator arteries showed origin from the anterior division in 53 cases (65%), from the inferior epigastric artery in 21 (26%; **Fig 5a**), from the posterior division in three (4%), and indirectly from the anterior division (with a common segment with the uterine artery) in four (5%; **Fig 5b**).

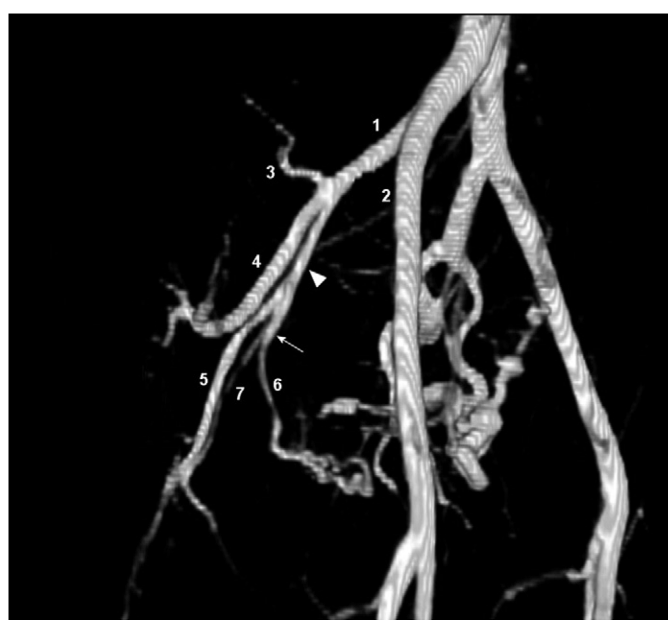

**Figure 3.** Three-dimensional reconstructed CE MR angiography image from the preembolization study of a 48-year-old woman. The model was rotated toward the left side for better visualization of the arteries on the right side, namely the IIA (*1*) with its anterior division (arrowhead), external iliac artery (*2*), iliolumbar artery (*3*), superior gluteal artery (*4*), inferior gluteal artery (*5*), and uterine artery (*6*) originating indirectly from the anterior division by a common segment (arrow) with the internal pudendal artery (*7*).

## DISCUSSION

The increased popularity of interventional procedures, many of which are based on the arterial system, and the introduction of high-technology noninvasive imaging techniques such as CT angiography and MR angiography, have allowed radiologists to study the arterial system in more detail with the aim of planning interventional procedures, providing the clinician or surgeon with details about vascular disease conditions or data that are considered crucial before surgical procedures. One of the most widely performed interventional procedures is UAE, which has emerged as a strong alternative to surgical options.

UAE has been widely recognized as a safe and effective treatment for symptomatic uterine leiomyomas (14–16) and an alternative to major surgery, including hysterectomy and myomectomy, because this minimally invasive treatment can contribute to improved symptoms with few major complications (17). It leads to impressive midterm and long-term improvement of all investigated physical and psychologic leiomyoma-related and -associated symptoms and significantly improves women's health-related quality of life (18). In addition, UAE can be used in combination with multiple myomectomy as a preoperative procedure to reduce the bleeding associated with the myomectomy operation. The target of this study was to

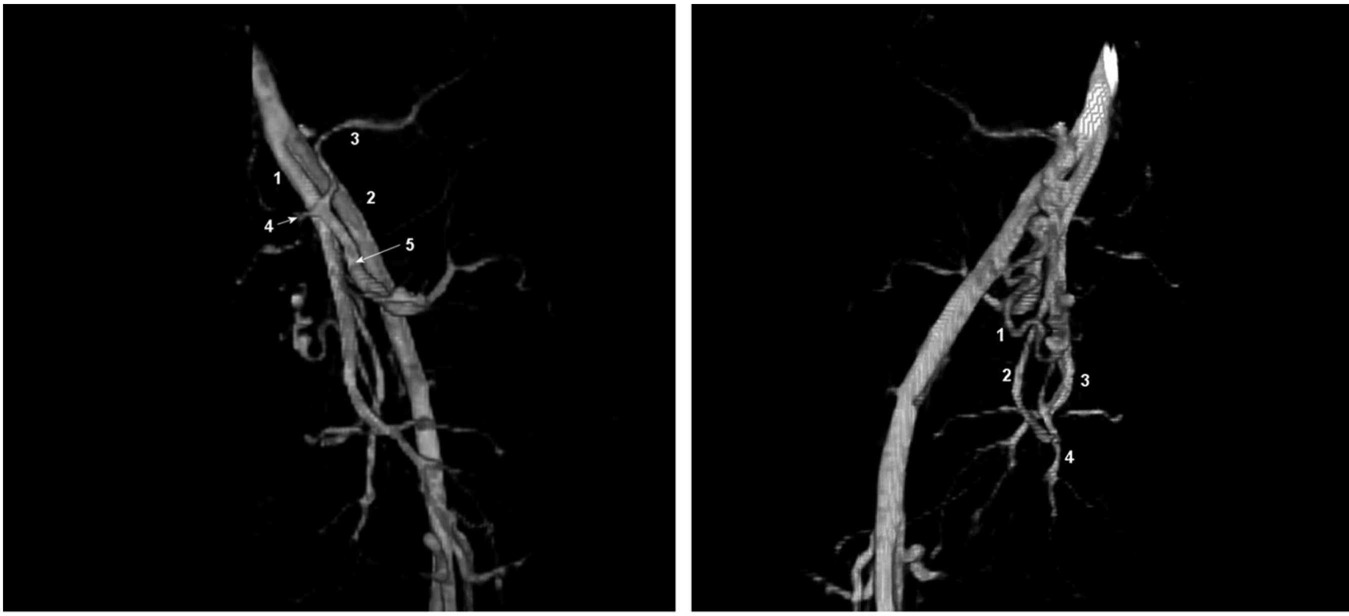


a. b.

**Figure 4.** **(a)** Three-dimensional reconstructed CE MR angiography image from the preembolization study of a 51-year-old woman. Direct posterior view with masking of the internal and external iliac arteries on the left side for better visualization of the branches of the posterior division of the IIA on the right side. This view shows the IIA (*1*), external iliac artery (*2*), iliolumbar artery (*3*), lateral sacral artery (*4*) before it divides into a superior and inferior divisions, and superior gluteal artery (*5*). **(b)** Another view from the same patient with masking of the IIA and external iliac artery on the left side and rotation of the 3D model toward the right side for better visualization of the branches of the anterior division of the right IIA. This view shows the uterine artery (*1*) with its characteristic tortuous appearance, superior vesical artery (*2*), inferior gluteal artery (*3*), and internal pudendal artery (*4*).

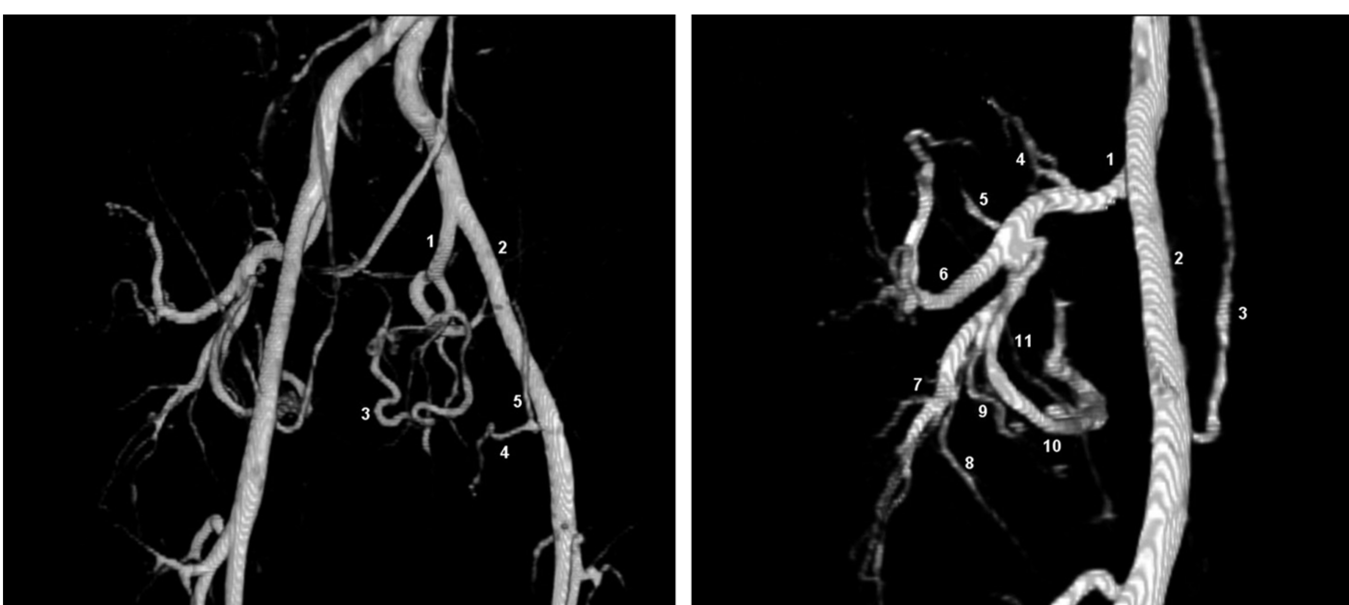


a. b.

**Figure 5.** **(a)** Three-dimensional reconstructed CE MR angiography image from the preembolization study of a 38-year-old woman. The 3D model was rotated toward the left side for better visualization of the arteries on the left side, namely the IIA (*1*), external iliac artery (*2*), uterine artery (*3*), and obturator artery (*4*), which originates from the inferior epigastric branch (*5*) of the external iliac artery. **(b)** Another view from the same patient with masking of the IIA and external iliac artery on the left side and rotation of the 3D model toward the left side for better visualization of the arteries on the right side, namely the IIA (*1*), external iliac artery (*2*) with its inferior epigastric branch (*3*), iliolumbar artery (*4*), lateral sacral artery (*5*), superior gluteal artery (*6*), inferior gluteal artery (*7*), internal pudendal artery (*8*), middle rectal artery (*9*), and uterine artery (*10*), which originates indirectly from the anterior division by a common segment with the obturator artery (*11*).

asses the ability of 3D reconstructed CE MR angiography in mapping the pelvic arterial tree in patients who underwent UAE.

CE MR angiography is a versatile technique that combines speed, superb contrast, and relative simplicity. It has a wide range of applications, particularly in the abdomen and pelvis (19). First, we tried to use the maximum-intensity projection images for the current study, and, despite the fact that it is the most common means of displaying the data from MR angiography studies, it did not supply us with full details regarding the IIA branches. This is probably because of the special nature of the IIA and its branches, with their long courses and obliquities necessitating visualization of the whole artery to allow correct identification, especially in the absence of bony landmarks. During routine angiographic procedures, identification of the IIA branches is facilitated if bony landmarks are established (20). As a result, the subtracted CE MR angiography images obtained were reconstructed with use of the Syngo Vessel-View application (the application used for 3D reconstruction of CT angiographic images), which provided a 3D model of the pelvic arterial tree that can be freely rotated and examined in all planes and directions, enabling the reader to completely trace the visualized arteries with a considerable degree of confidence and clarity.

After evaluation, an attempt was made to correlate the 3D reconstructed CE MR angiography images with the angiographic images (the gold standard for arterial visualization), but the main problem was that the 3D model can be freely rotated in any direction to see each branch and trace it separately, whereas angiography was performed with the aim of visualizing the origin of the uterine artery to enter it with the catheter. Because the study was done in a retrospective manner, it was very difficult to find the projection among a patient's angiographic images that coincided with the rotated 3D reconstructed model, except in some rare circumstances (**Fig 2**).

It was observed that 3D reconstructed CE MR angiography was sensitive in detecting the major parietal branches, namely the superior and inferior gluteal and internal pudendal arteries, probably because their relatively large diameter and parietal course away from the pelvic viscera allows improved enhancement and clear visualization. Regarding the other parietal branches—namely the lateral sacral, iliolumbar, and obturator arteries—CE MR angiography showed them with relatively high sensitivity. Regarding the visceral branches, the uterine artery was the only artery detected in a high percentage of cases, which is probably related to its characteristic tortuous course and large diameter in patients with uterine leiomyomas, in whom it is enlarged to supply the tumors. The other two included visceral branches, namely the superior vesical and middle rectal arteries, were detected in a relatively small number of patients, most likely because of their small diameter and course within the pelvic cavity.

Regarding the lengths of the detectable branches of the IIA, the uterine artery showed the longest detectable lengths, probably because of its inherent tortuosity and enlargement in patient with uterine leiomyomas; this was followed by the internal pudendal and obturator arteries, likely attributed to the fact that these two arteries travel for a long distance before giving off their first branch. Conversely, some other arteries known to divide immediately after their origin—such as the lateral sacral artery dividing immediately into superior and inferior branches or the iliolumbar artery dividing into ilial and lumbar branches—showed the least detectable lengths.

Previously, several studies have tried to classify the pattern of branching of the IIA and the modes of origin of its different branches (21,22). In fact, the pattern of division of the IIA is beyond the scope of our study, as we tried to focus mainly on the uterine artery, the target artery in uterine leiomyoma treatment. In addition, special attention was given to the obturator artery because of its surgical importance.

The current study identified five points of origins of the uterine artery. The most common was a direct origin from the anterior division seen in 90% of cases, followed by an indirect origin from the anterior division with a short trunk with other arteries seen in five arteries, four with the obturator and one with the internal pudendal artery. We identified another two patterns of origin, one from the main stem of the IIA and the other from the point of its bifurcation. The latter was grouped alone because we thought it would have an impact on the embolization procedure, in which a relatively small artery is selected at the point of bifurcation of a major artery, which constitutes a challenge to the interventionist. Another single rare incidence was an origin from the posterior division; this constitutes a critical condition because the posterior division, according to Greenwood et al (23), must be preserved during the embolization procedure. These results partially agree with those of Pelage et al (20), who identified a single origin of the uterine artery from the anterior division of the IIA; we believe this origin is the most common, but not the sole pattern of origin.

The second artery of special concern to us was the obturator artery. Despite the fact that it is unrelated to the UAE procedure, it has a special surgical importance and the traditional surgical teaching warns of the danger of dissecting blindly along the iliopectineal line for fear of lacerating the "Crown of Death" (this refers to an aberrantly originating obturator artery taking origin from the inferior epigastric artery and crossing over the pelvic rim). In the current study, the obturator artery showed four patterns of origin, the most common of which was a direct origin from the anterior division. Other origins include an indirect origin from the anterior division with a common trunk with other arteries (the uterine artery), the posterior division, and finally the inferior epigastric artery, which was seen in 26% of examined arteries. According to Gilory et al (24), the incidences of a sole obturator artery in the variant position (originating from the inferior epigastric/external iliac artery) were 22% in specimens in the United States and 10% in specimens in China.

Limitations of the current study include the performance of the study in one group of women (those with uterine leiomyomas), which has an impact on the size and consequently the visualization of the uterine artery. A second limitation is the lack of comparison between the 3D rotational MR angiographic reconstructions and digital subtraction angiography or 3D rotational digital subtraction angiography.

We regard the present study as a step on a long road of usage of 3D imaging in diagnostic and interventional procedures, especially in the presence of newly introduced technologies such as C-arm CT (25), 3D rotational angiography (26), and 3D road mapping (27), all of which hold promise for the future.

We conclude that 3D reconstructed CE MR angiography can detect most branches of the IIA in women, in addition to the branches' points of origin. Such information might be of help before pelvic interventional procedures, especially UAE, which requires a good knowledge of the anatomy to ensure the delivery of a safe procedure and avoid nontarget embolization. Still, a similar study, conducted in a prospective manner, is required to evaluate the real impact of such findings on the interventional procedure itself.

**References**


1. Flanigan DP, Sobinsky KR, Schuler JJ. Internal iliac artery revascularization in the treatment of vasculogenic impotence. Arch Surg 1985; 120:271–274.
2. Elsharawy MA, Cheatle TR. Buttock claudication secondary to isolated internal iliac artery stenosis. Eur J Vasc Endovasc Surg 2000; 19:87–89.
3. Fernandez H, Pons JC, Chambon G, Frydman R, Papiernik E. Internal iliac artery ligation in post-partum hemorrhage. Eur J Obstet Gynecol Reprod Biol 1988; 28:213–220.
4. Chou MM, Hwang JI, Tseng JJ, Ho ES. Internal iliac artery embolization before hysterectomy for placenta accreta. J Vasc Interv Radiol 2003; 14: 1195–1199.
5. Kickuth R, Dick F, Triller J, Ludwig K, Schmidli J, Do DD. Internal iliac artery embolization before endovascular repair of aortoiliac aneurysms with a nitinol vascular occlusion plug. J Vasc Interv Radiol 2007; 18:1081–1087.
6. Engelke C, Elford J, Morgan RA, Belli AM. Internal iliac artery embolization with bilateral occlusion before endovascular aortoiliac aneurysm repair-clinical outcome of simultaneous and sequential intervention. J Vasc Interv Radiol 2002; 13:667–676.
7. Wolpert LM, Dittrich KP, Hallisey MJ, et al. Hypogastric artery embolization in endovascular abdominal aortic aneurysm repair. J Vasc Surg 2001; 33: 1193–1198.
8. Mishell DR, Stenchever MA, Droegemuller W, Herbst AL. Comprehensive gynecology, 3rd ed. St. Louis: Mosby-Year Book, 1997; 484–488.
9. Subramanian S, Spies JB. Uterine artery embolization for leiomyomata: resource use and cost estimation. J Vasc Interv Radiol 2001; 12:571–574.
10. Chrisman HB, Minocha J, Ryu RK, Vogelzang RL, Nikolaidis P, Omary RA. Uterine artery embolization: a treatment option for symptomatic fibroids in postmenopausal women. J Vasc Interv Radiol 2007; 18:451–454.
11. Spies JB, Sacks D. Credentials for uterine artery embolization. J Vasc Interv Radiol 2004; 15:111–113.
12. Dueholm M, Lundorf E, Hansen ES, Ledertoug S, Olesen F. Accuracy of magnetic resonance imaging and transvaginal ultrasonography in the diagnosis, mapping, and measurement of uterine myomas. Am J Obstet Gynecol 2002; 186:409–415.
13. Omary RA, Vasireddy S, Chrisman HB, et al. The effect of pelvic MR Imaging on the diagnosis and treatment of women with presumed symptomatic uterine fibroids. J Vasc Interv Radiol 2002; 13:1149–1153.
14. Spies JB, Ascher SA, Roth AR, Kim J, Levy EB, Gomez-Jorge J. Uterine artery embolization for leiomyomata. Obstet Gynecol 2001; 98:29–34.
15. Vogl TJ, Jacobi V, Gätje R, Siebzehnrübl E, Zangos S. Embolization of symptomatic myomas (UAE): technique, indication and results. Fortschr Rontgenstr 2003; 175:1032–1041.
16. Worthington-Kirsch RL. Uterine artery embolization for fibroid disease is not experimental. Cardiovasc Intervent Radiol 2005; 28:148–149.
17. Katsumori T, Kasahara T, Akazawa K. Long-Term outcomes of uterine artery embolization using gelatin sponge particles alone for symptomatic fibroids. AJR Am J Roentgenol 2006; 186:848–854.
18. Bucek RA, Puchner S, Lammer J. Mid- and long-term quality-of-life assessment in patients undergoing uterine fibroid embolization. AJR Am J Roentgenol 2006; 186:877–882.
19. Glockner JF. Three-dimensional Gadolinium-enhanced MR angiography: applications for abdominal imaging. Radiographics 2001; 21:357–370.
20. Pelage JP, Le Dref O, Soyer P, et al. Arterial anatomy of the female genital tract: variations and relevance to transcatheter embolization of the uterus. AJR Am J Roentgenol 1999; 172:989–994.
21. Adachi B. Das Arteriensystem der Japaner bd. II. Kyoto. Suppl Acta Schol Med Univ Imperialis Kyoto 1927; 9:95–125.
22. Jastschinski S. Die typischen verzweigsform der arteria hypogastrica. Int Mschr Anat Physiol 1891; 8:111–127.
23. Greenwood LH, Glickman MG, Schwartz PE, Morse SS, Deny DE. Obstetric and nonmalignant gynecologic bleeding: treatment with angiographic embolization. Radiology 1987; 164:155–159.
24. Gilory AM, Hermey DC, Dibenedetto LM, Marks SC, Page DW, Lei QF. Variability of the obturator vessels. Clin Anat 1997; 10:328–332.
25. Wallace MJ, Murthy R, Kamat PP, et al. Impact of C-arm CT on hepatic arterial interventions for hepatic malignancies. J Vasc Interv Radiol 2007; 18:1500–1507.
26. Liapi E, Hong K, Georgiades CS, Geschwind JF. Three-dimensional rotational angiography: introduction of an adjunctive tool for successful transarterial chemoembolization. J Vasc Interv Radiol 2005; 16:1241–1245.
27. Söderman M, Babic D, Homan R, Andersson T. 3D roadmap in neuroangiography: technique and clinical interest. Neuroradiology 2005; 47:735–740.